S E S 2 0 1 9
Fifteenth International Scientific Conference
SPACE, ECOLOGY, SAFETY
6 – 8 November 2019, Sofia, Bulgaria

SOLAR ORIGIN OF COMMON INTERANNUAL CYCLES OF EARTH ROTATION, MSL AND CLIMATE

Yavor Chapanov[1], Cyril Ron[2], Jan Vondràk[2]

[1]Climate, Atmosphere and Water Research Institute – Bulgarian Academy of Sciences
[2]Astronomical Institute – Czech Academy of Sciences
e-mail: yavor.chapanov@gmail.com; ron@ig.cas.cz; vondrak@ig.cas.cz

Keywords: *solar activity, TSI, SSN, MSL, LOD, climate*

Abstract: *The solar activity cycles affect all surface geosystems, including weather and climate indices, winds, rains, snow covers, mean sea level (MSL), river flowing and other hydrological cycles. The MSL and polar ice changes cause common variations of the principal moments of inertia and consequently also the Earth rotation with decadal, centennial and millennial periods. The MSL, Earth rotation and climate indices have also some oscillations with periods from several months to 10 years, whose origin is not connected with the known tidal, seasonal and other Earth effects. The shape of solar cycles is rather different from sinusoidal form, so they affect geosystems by many short-term harmonics. The solar origin of interannual oscillation of Earth rotation, MSL and climate indices is investigated by long time series of Length of Day (LOD), MSL variations at Stockholm, temperature and precipitation over South-Eastern Europe, El-Nino Southern Oscillation (ENSO), Total Solar Irradiance (TSI), sunspot numbers SSN and North-South solar asymmetry (N-S SA).*

Introduction

The Sun is the main energy source for all surface geosystems, including climate, weather, MSL, winds, rainfalls etc. The essential energy transfer from the Sun to the Earth is the Total Solar Irradiance (TSI) whose variations during the solar activity cycles cause various changes on the Earth surface. The global energy balance (Fig. 1) consists of incoming and outgoing radiation [1]. The part of incoming solar radiation is reflected back and the rest is absorbed by surface and atmosphere.

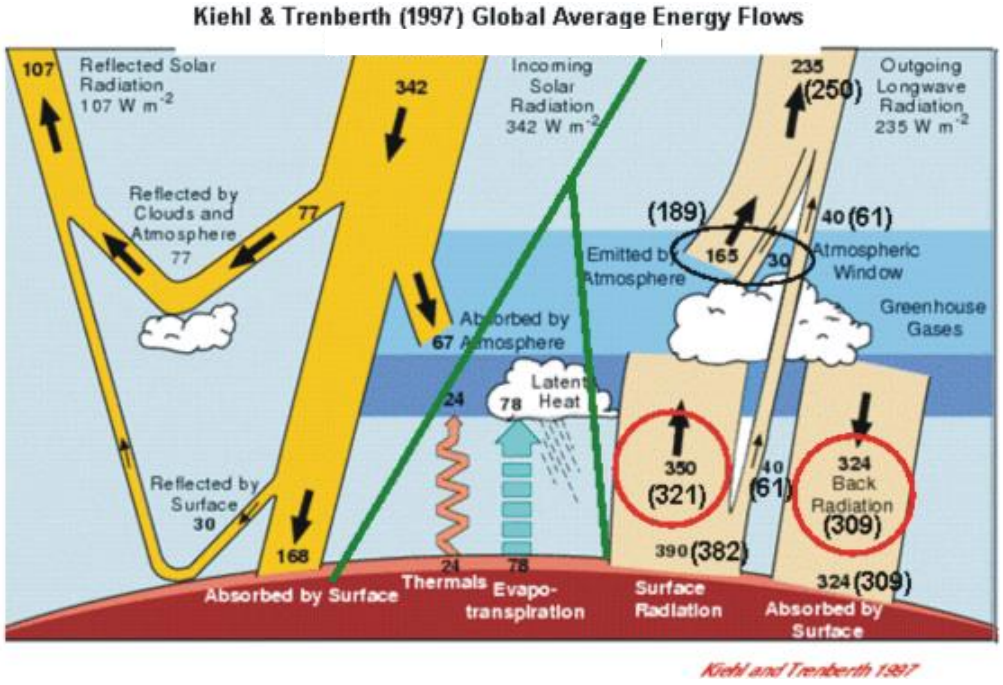

Fig. 1. The global energy balance according Kiehl and Trenberth (1997)

A part of absorbed by surface solar radiation produces evapotranspiration mainly from ocean. Another part of the absorbed solar radiation produces global atmosphere circulation. This circulation transport a part of evaporated ocean water from equatorial to polar regions by Hadley, Ferrel and polar cells (Fig. 2). Any change of the incoming solar radiation leads to variations of evaporated ocean water and water transport from equatorial regions to polar ice. So in case of common increase of polar ice thickness, the mean sea level decreases and vice versa.

The climate, MSL, and polar ice thickness response to the solar activity and thus consist of cycles whose periods are close to the well-known solar decadal, centennial and millennial periods and their higher harmonics. The TSI variations significantly affect water evaporation and global water cycles. The global water redistribution between the oceans and continental polar ice leads to periodical changes of the principal moment of inertia C, followed by the Earth rotation variations, according to the law of the angular momentum conservation. The strong local variations of precipitation due to solar cycles affect river streamflows and possible floods.

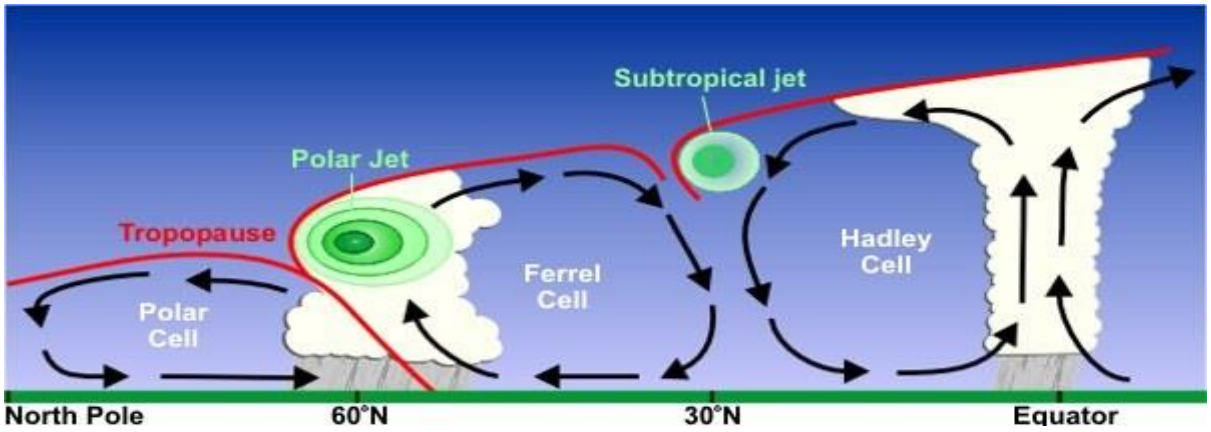

Fig. 2. Circulation patterns in Hadley, Ferrel, and polar cells, according NOAA

Data and Methods

The daily values of SSN for the period 1818.0-now are provided by the Royal Observatory of Belgium. The time series of the TSI for the period 1610.5-2000.5 are reconstructed in [2]. The Earth rotation data for the period 1623.5–2005.5 are available from the IERS EOP Data Center. The detrended values of the MSL at Stockholm are determined in [3]. The annual time series of LOD are combination between the solution of Stephenson and Morrison [4], based on lunar eclipses and star occultations before 1955 and modern determinations afterwards. Another denser time series is the solution C02 of IERS 1830-now.

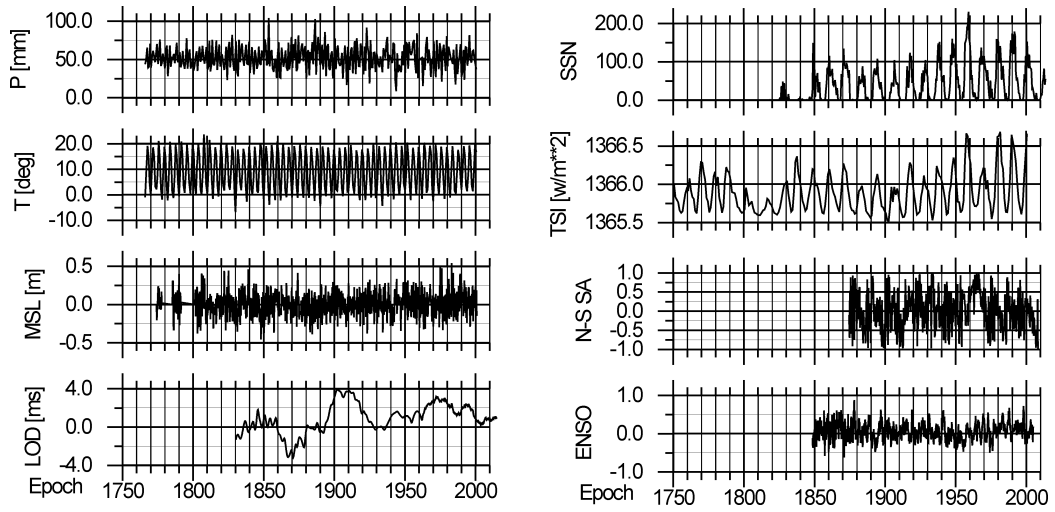

Fig. 3. Time series of precipitation P, temperature T over South-Eastern Europe, MSL, LOD, SSN, TSI, ENSO and N-S solar asymmetry

The ENSO monthly data since 1817 are available at the WEB page of the Joint Institute for the Study of the Atmosphere and Ocean http://research.jisao.washington.edu/data/globalsstenso/. The North-South solar asymmetry is determined from the relation $(S_n–S_s)/(S_n+S_s)$, where the S_n and S_s are monthly sunspot area on the Northern and Southern solar hemispheres, respectively (in units of millionths of a hemisphere). The data since 1874 are observed by the Royal Greenwich Observatory and merged after 1976 with the US Air Force (USAF) and the US National Oceanic and Atmospheric Administration (NOAA) data by D. Hathaway (https://solarscience.msfc.nasa.gov/greenwch.shtml).

The precipitation and temperature over part of Eastern Europe for the period 1767–2000 are determined from the gridded data [5, 6]. The climatic data of part of Eastern Europe between 11°– 30 °E and 41°– 51 °N are determined from 710 grids (0.5° x 0.5°) over the ground (Fig. 4). The monthly temperature and precipitation are averaged from their gridded values by the robust Danish Method. The Danish Method [7–9] provides robust estimation of mean values and eliminates all data outliers.

Fig. 4. Map of South-Eastern Europe

The periodical variations are derived from the data by means of Partial Fourier Approximation based on the Least-Squares (LS) estimation of Fourier coefficients. The Partial Fourier Approximation $F(t)$ of discrete data is given by

$$F(t) = f_0 + f_1(t-t_0) + \sum_{k=1}^{n} a_k \sin k\frac{2\pi}{P_0}(t-t_0) + b_k \cos k\frac{2\pi}{P_0}(t-t_0), \quad (1)$$

where P_0 is the period of the first harmonic, t_0 - the mean epochs of observations, f_0, f_1, a_k and b_k are unknown coefficients and n is the number of harmonics of the partial sum, which covers all oscillations with periods between P_0/n and P_0. The application of the LS estimation of Fourier coefficients needs at least $2n + 2$ observations, so the number of harmonics n is chosen significantly smaller than the number N of sampled data f_i. It should be kept in mind that the small number of harmonics n yields to LS estimation of the coefficient errors, too. This estimation is the first essential difference with the classical Fourier approximation. The second essential difference with the classical case is the arbitrary choice of the period of first harmonic P_0, instead of the observational time span, so the estimated frequencies may cover the desired set of real oscillations. This method allows a flexible and easy separation of harmonic oscillations into different frequency bands by the formula:

$$B(t) = \sum_{k=m_1}^{m_2} a_k \sin k\frac{2\pi}{P_0}(t-t_0) + b_k \cos k\frac{2\pi}{P_0}(t-t_0), \quad (2)$$

where the desired frequencies ω_k are limited by the bandwidth

$$\frac{2\pi m_1}{P_0} \le \omega_k \le \frac{2\pi m_2}{P_0}, \quad (3)$$

After estimating the Fourier coefficients, it is possible to identify a narrow frequency zone presenting significant amplitude, and defining a given cycle. Then this cycle can be reconstructed in time domain as the partial sum limited to the corresponding frequency bandwidth. Doing this for terrestrial and solar time series we shall identify their respective cycles, isolate and compare the common ones.

The common solar and terrestrial cycles are derived by a model of harmonic oscillations with three different group of oscillations. The main group of oscillations is born by the 22-year solar cycle and its 22 harmonics. They cover all periods from 1 to 22 years (Table1). The used solar and terrestrial time series have different long-periodical behavior and their long-term variations with decadal periods are eliminated by the first 10 harmonics of 125-year oscillation (Table 2). The 5-th, 6-th and 7-th harmonics of these long terms are excluded from the model, because the beat period between them, the lunar node and the 22-year solar cycle is greater than the 125-year observational span. The terrestrial data are affected by different long term tides, while the solar data are not, so it is necessary to eliminate any oscillations with the periods of long term tides between 1 and 18.6 years. To do this, the model of common interannual solar-terrestrial cycles includes additional 6 oscillations with tidal periods (Table 3). The model of common interannual solar-terrestrial cycles consists of the above groups of tidal oscillations, long period terms and solar harmonics. The harmonic coefficients of this model are estimated by means of the Method of Partial Fourier Approximation. The estimation accuracy is better than 30μs for LOD; 1 for SSN; 0.01W/m^2 for TSI; 7mm for MSL; 0.01 for ENSO; 0.02 for N-S solar asymmetry, 0.07° for temperature T; and 0.8mm for precipitation P.

Table 1. Harmonics of 22-year solar cycle

No	Period [yr]	No	Period [yr]
1	22.00	12	1.83
2	11.50	13	1.69
3	7.33	14	1.57
4	5.50	15	1.47
5	4.40	16	1.37
6	3.67	17	1.29
7	3.14	18	1.22
8	2.75	19	1.16
9	2.44	20	1.10
10	2.20	21	1.05
11	2.00	22	1.00

Table 2. Harmonics of 125-year period

No	Period [yr]
1	125.00
2	62.50
3	41.67
4	31.25
8	15.62
9	13.89
10	12.50

Table 3. Fundamental terms and periods of long term tides

l	l'	F	D	Ω	Period [days]
1	0	0	–1	0	411.78
2	0	–2	0	0	–1095.18
–2	0	2	0	1	1305.48
–1	1	0	1	0	3232.86
0	0	0	0	2	–3399.19
0	0	0	0	1	–6798.38

Results

The common cycles between solar and terrestrial indices are calculated by the Method of Partial Fourier Approximation and the Model of 22-year oscillations according Tables 1–3. These cycles are shown in Figs. 5–8. They cover several bands with periodicities between 1.04 and 7.3 yr. The MSL have good correlation with SSN variations (Fig. 5). The LOD is affected by SSN and TSI variations (Fig. 6). The ENSO correlate with the N-S solar asymmetry (Fig. 7). The temperature is affected by the TSI variations, while the precipitation – by SSN variations (Fig. 8). Some common cycles have phase reverse for short-time intervals.

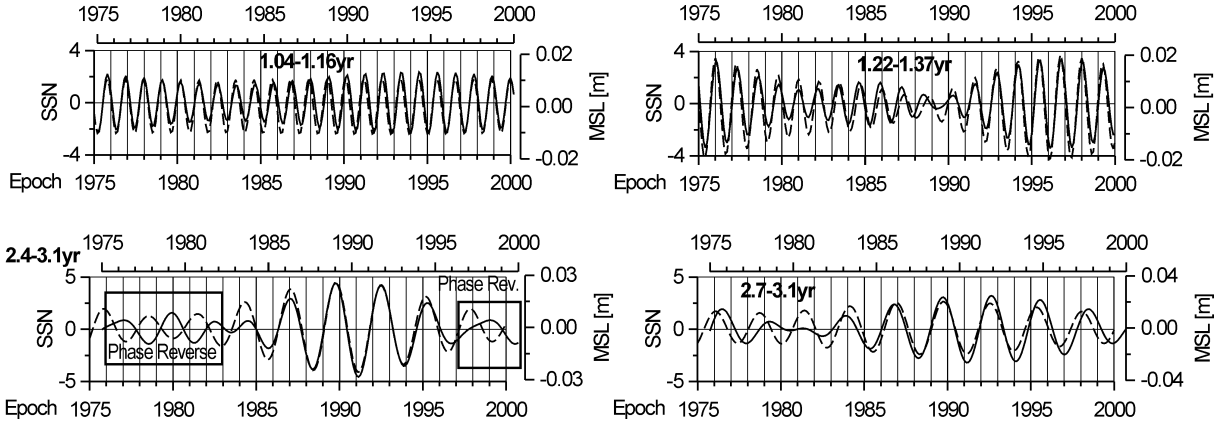

Fig. 5. Solar influence on MSL (dashed line) interannual variations

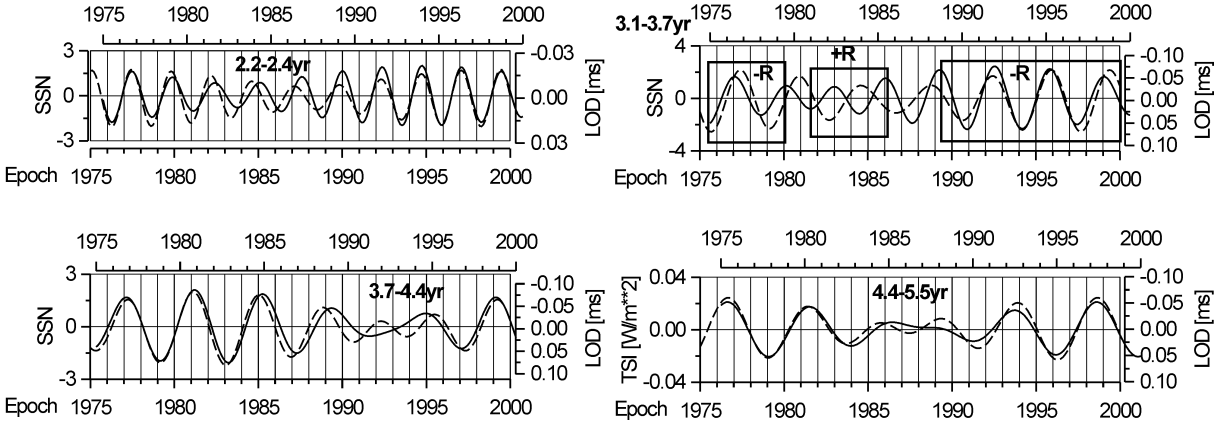

Fig. 6. Solar influence on LOD (dashed line) interannual variations

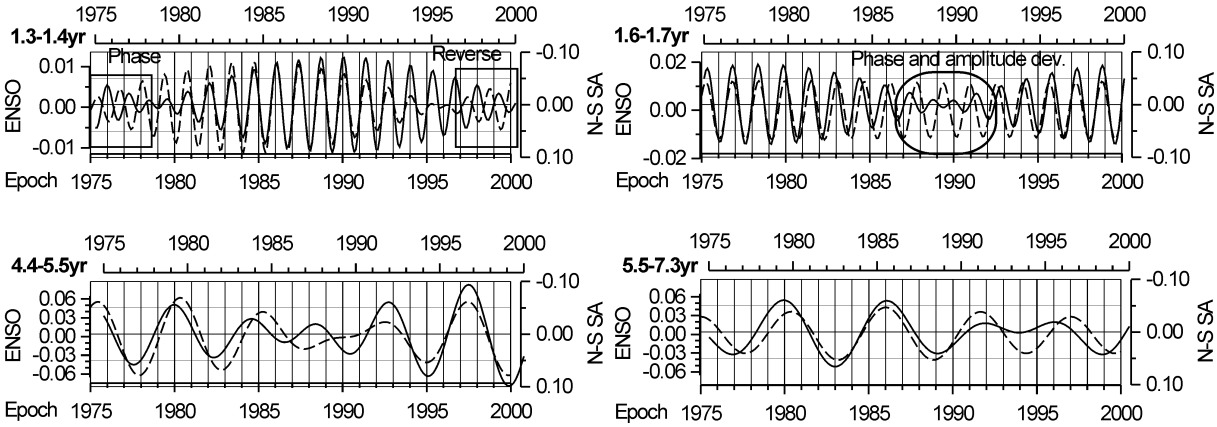

Fig. 7. Solar influence on ENSO (dashed line) interannual variations

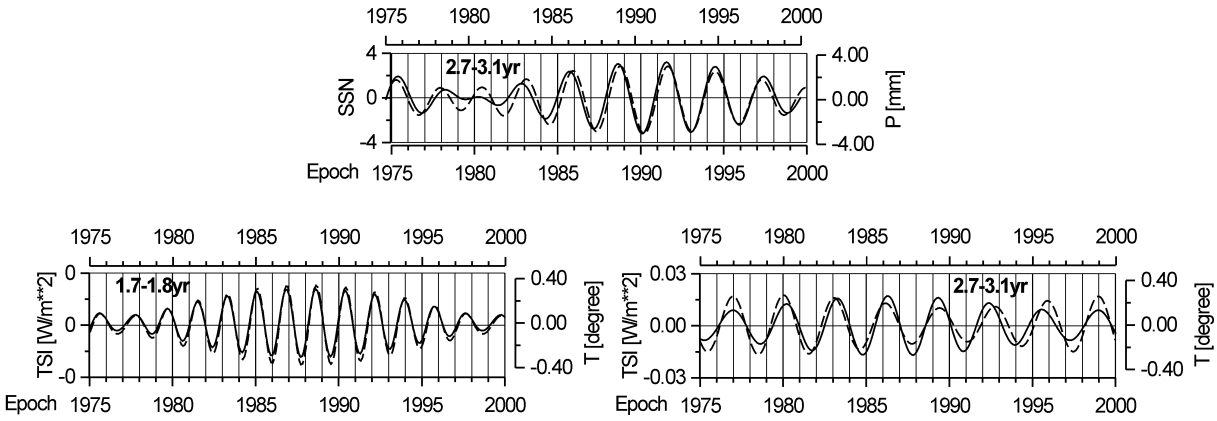

Fig. 8. Solar influence on T and P (dashed line) interannual variations

The common interannual solar-terrestrial cycles are determined by superposition of two oscillations with neighbor periods from Table 1 and their comparison. The variations of the Wolf's numbers represent mainly the intensity of the solar wind. The solar wind variations affect interplanetary and Earth magnetic fields, whose changes modulate the cosmic rays. The cosmic rays produce a ionization of the atmosphere, changes of atmosphere conductivity, lightning, and an increase of ozone concentration. The changes of atmospheric water vapor content and ozone plays significant role in climate variations. The SSN strongly affect earth rotation, mean sea level and precipitation over South-Eastern Europe (Figs. 5, 6, 8), whose variations are connected with climate changes. The total solar irradiance affects climate changes directly. The TSI variations have good agreement with LOD and temperature over Eastern Europe (Fig. 8). The N-S solar asymmetry is connected with solar magnetic field disturbances, followed by temporal variations of solar wind and corresponding changes of the heliosphere and these processes produce modulation of cosmic rays, so the solar cycles may drive Enso variations by modulation of cosmic rays over the Pacific Ocean. The chosen examples of common interannual solar-terrestrial cycles in Figs. 5–8 expose identical variations of amplitudes and phases.

Conclusions

The investigation of the variations of Earth parameters in time and their connection with solar activity is very important in studying the natural risks and the environmental changes. The new complex local and global models of solar-terrestrial interconnections may improve long term forecasts of danger climate events like severe dry or wet, floods, extremely high or low temperatures. The existing long climatic and astronomical time series with centennial time spans are useful to study common decadal and centennial cycles of the solar activity, climate, Earth rotation and other terrestrial phenomena. The solar activity affects all geosystems by its decadal, centennial and millennial cycles and especially by their harmonics, due to non-sinusoidal shapes of the known cycles. A good agreement exists between the interannual cycles of LOD, MSL, climate and solar indices whose periods are between 1 and 7.3 years. Chapanov et al. determine common decadal cycles of Earth rotation, mean sea level and climate, excited by solar activity harmonics [10]. New frequency bands of common interannual cycles in solar, climatic and geodetic data are determined by means of solar harmonics. The new linear models of common cycles with periods from several months to 50 years in solar, climatic and geodetic data may improve our knowledge of solar-terrestrial influences. It is possible to create long-term forecasts of climate change, mean sea level and Earth rotation variations with high resolution in time.

References:

1. Kiehl, J. T. and K. E. Trenberth, Earth's annual global mean energy budget, Bulletin of the American Meteorological Society, 78, 1997, 197–208. doi10.1175/1520-0477(1997)0782.0.CO;2.
2. Lean, J., Evolution of the Sun's spectral irradiance since the Maunder Minimum, Geophysical Research Letters, 27, 16, 2000, 2425–2428.
3. Ekman, M., The world's longest sea level series and a winter oscillation index for northern Europe 1774 - 2000, Small Publications in Historical Geophysics, 2003, 12, 31 p.
4. Stephenson, F. R. and L. V. Morrison, Long-term changes in the rotation of the Earth: 700 BC to AD 1980, Philosophical Transactions of the Royal Society of London, Ser. A, 4770, 1984.
5. Casty, C., D. Handorf, and M. Sempf, Combined climate winter regimes over the North Atlantic/European sector 1766–2000, Geophys. Res. Letters, 32, 13, 2005, DOI: 10.1029/2005GL022431 C.
6. Casty, C., C.C. Raible, T.F. Stocker, J. Luterbacher, and H. Wanner, A European pattern climatology 1766-2000, Climate Dynamics, 29, 7, 2007, 791-805. DOI: 10.1007/s00382-007-0257-6.
7. Juhl, J.: The Danish Method of weight reduction for gross error detection. XV ISP Congress Proc., Comm. III, Rio de Janeiro, 1984.
8. Kegel, J.: Zur Lokalizierung grober Datenfehler mit Hilfe robuster Ausgleichungsfervahren. Vermes-sungstechnik, 35, 10, Berlin, 1987.
9. Kubik, K.: An error theory for the Danish method. ISP Symposium, Comm. III, Helsinki, 1982.
10. Chapanov Y., C. Ron, J. Vondrk, Decadal cycles of Earth rotation, mean sea level and climate, excited by solar activity, Acta Geodyn.Geomater., 14, No. 2 (186), 2017, 241–250, DOI:10.13168/AGG.2017.0007